(9) "Gmelin's Handbuch der Anorganischen Chemie, Iron 59B," Verlag Chemie, Gmbh, Berlin, Germany, 1938, p. 903.
(10) O. Baudisch, *Science*, **108**, 443(1948).
(11) W. P. Griffith, *Quart. Rev.*, **16**, 188(1962).
(12) E. F. Hockings and I. Bernal, *J. Chem. Soc.*, **1964**, 5029.
(13) J. D. W. VanVoorst and P. Hemmerich, *J. Chem. Phys.*, **45**, 3914(1966).
(14) J. B. Raynor, *Nature*, **201**, 1216(1964).
(15) J. Dempir and J. Masek, *Inorg. Chim. Acta*, **2**, 402(1968).
(16) J. H. Swinehart and P. A. Rock, *Inorg. Chem.*, **5**, 573(1966).
(17) P. P. Mitra, D. V. S. Juin, A. K. Banerjee, and K. V. R. Chari, *J. Inorg. Nucl. Chem.*, **25**, 1263(1963).
(18) B. Joselskis and J. C. Edwards, *Anal. Chem.*, **32**, 381(1960).
(19) T. Martin and J. A. Patel, *Amer. J. Hosp. Pharm.*, **26**, 51(1969).
(20) I. H. Page, *J. Amer. Med. Ass.*, **147**, 1311(1951).
(21) L. Lachman, C. J. Swartz, and J. Cooper, *J. Amer. Pharm. Ass., Sci. Ed.*, **49**, 213(1960).
(22) F. A. Cotton, R. R. Monchamp, R. J. M. Henry, and R. C. Young, *J. Inorg. Nucl. Chem.*, **7**, 32(1958).

ACKNOWLEDGMENTS AND ADDRESSES

Received December 23, 1974, from *Hoffmann-La Roche, Inc., Nutley, NJ 07110*

Accepted for publication April 1, 1975.

The authors are indebted to Mr. Vincent Rizzo for preparation of anhydrous, lyophilized sodium nitroprusside and to Ms. Mildred Sarli for drawing the figures.

[x] To whom inquiries should be directed.

Effect of Solvent Flow Reynolds Number on Dissolution Rate of a Nondisintegrating Solid (Potassium Chloride)

J. VALERIE FEE [x], D. J. W. GRANT [x], and J. M. NEWTON

Abstract □ An apparatus for measuring dissolution rates of solids in the form of disks was designed to possess the following features. The solvent flowed continuously and reproducibly past the disk at various rates associated with calculable Reynolds numbers, *Re*. The effluent solution was adequately mixed before analysis. The concentration of dissolved solute was much less than the solubility. The surface area of the disk in contact with the solvent was constant during measurements. The dissolution rate of the disk was reproducible, and the disk and its surface could be readily characterized. The apparatus was tested at 37° with compressed potassium chloride and water. The intrinsic dissolution rate, G, was a linear function of *Re* from *Re* = 360 to >6000. This relationship enabled one unknown constant in each dissolution theory to be expressed in terms of *Re*. For the diffusion layer model, the thickness of this layer, calculated from the experimental value of G, agreed well with that calculated from the various physical properties, provided that natural convection did not predominate. The dissolution of potassium chloride in this system was, therefore, controlled by diffusion.

Keyphrases □ Dissolution rates—solid nondisintegrating disk (potassium chloride), apparatus described, effect of solvent flow Reynolds number □ Solvent flow—Reynolds number, effect on dissolution rate of nondisintegrating solid disk (potassium chloride) □ Reynolds number—effect on dissolution rate of nondisintegrating potassium chloride solid disk, apparatus described and evaluated

The first major objective of this work was to design, construct, and test an apparatus with the following features for determining the dissolution rate of solids.

(*a*) The solvent flow in the apparatus should be controlled and characterized by a calculable value of the Reynolds number, *Re*.

(*b*) The effluent solution from the apparatus should be adequately mixed before analysis.

(*c*) The concentration, c, of dissolved solute must be much less than the solubility, c_s, *i.e.*, $(c_s - c) \approx c_s$, or, in other words, sink conditions must apply.

(*d*) The surface area of the solid disk in contact with the dissolution medium must be constant.

(*e*) The dissolution rate of the solid must be reproducible.

(*f*) The solid disk and its surface must have reproducible properties that can readily be characterized.

(*g*) The solid surface should be positioned in the solvent stream so that the flow over the solid is reproducible.

The second major objective was to study how the intrinsic dissolution rate, G, of a solid substrate depends on the flow rate of the solvent and, therefore, on *Re*. The third major objective was to deduce which dissolution theory or model best fits the results and describes the dissolution process.

EXPERIMENTAL

Materials—The potassium chloride was spectroscopic grade[1], and the solvent in the dissolution experiments was glass-distilled water of very low potassium content (<0.01 mg/liter).

Preparation of Solid Disks—Transparent disks, 13 mm in diameter, 2 mm thick, and encircled by a 21-mm external diameter Nimonic[2] creep-resistant alloy ring (disk holder K), were prepared by compressing 315 mg of finely powdered potassium chloride at 10 tons load for 5 min under vacuum in a die and punch assembly (Fig. 1). The upper surface of the finished disk to be exposed to the solvent was level with the rim of the holder while the lower surface was recessed to enable it to fit on the raised knob on stub D in dissolution chamber C (Fig. 2).

Petroleum jelly was used for adhesion and ensured that the sol-

[1] B.D.H. Chemicals Ltd., Poole, Dorset, BH12 4NN, England.
[2] Henry Wiggin and Co. Ltd., Wiggin Street, Birmingham, England.

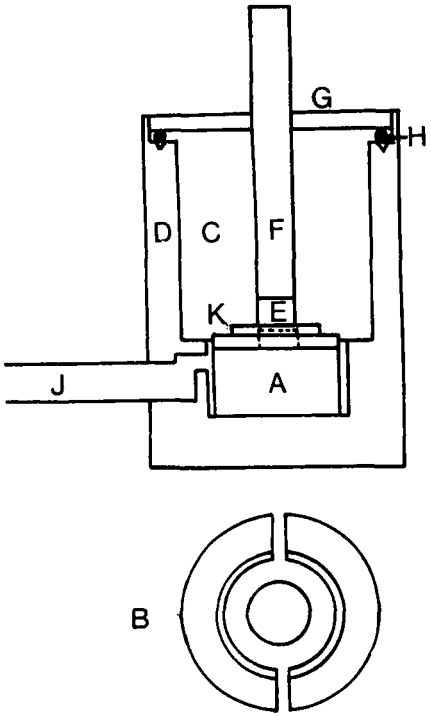

Figure 1—*Die and punch assembly for preparing compressed disks of potassium chloride (of mass 315 mg and diameter 13 mm) surrounded by a Nimonic alloy ring for dissolution experiments. Key: A, anvil; B, cylindrical recessed base of C; C, cylindrical barrel; D, die body; E, platen; F, plunger; G, die top; H, Neoprene O-ring seal; J, tube for connection to vacuum pump; and K, Nimonic alloy ring.*

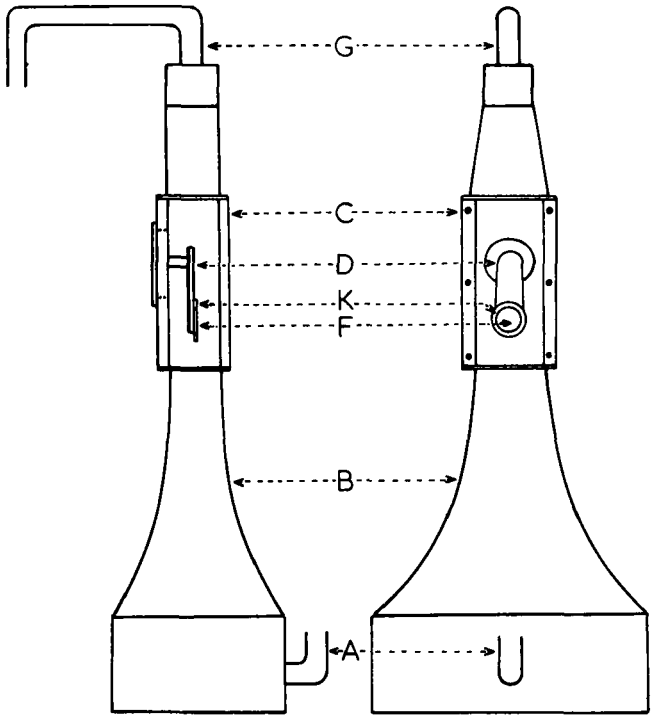

Figure 2—*Apparatus for determining the dissolution rate of a solid in a stream of flowing solvent (scale, approximately 0.23× actual size). Key: A, inlet tube from control valve and reservoirs; B, exponentially shaped horn; C, dissolution chamber; D, stub for fixing the disk holder; K, disk holder; F, solid disk of potassium chloride; and G, effluent tube.*

vent did not reach the hidden surface of the disk.

Dissolution Apparatus—The apparatus (Fig. 2) was constructed of stainless steel, except for one face of dissolution chamber C. This one face was of polymethyl methacrylate to enable the outer surface of the potassium chloride disk to be viewed. Stub D, carrying disk holder K, could be put into C and taken out of C through the back wall.

To produce uniform flow of solvent over the greatest possible cross-sectional area of dissolution chamber C, fluid was introduced through an exponentially shaped horn, B (Fig. 2). Such a system ensures a uniform flow velocity over the region beyond the hydrodynamic boundary layer adjacent to each wall (1) (Fig. 3). The thickness, h_0, of the hydrodynamic boundary layer can be calculated from:

$$h_0 \approx \frac{2.0x}{\sqrt{\frac{x\rho\bar{u}}{\eta}}} \qquad \text{(Eq. 1)}$$

where x is the length of the exponential horn (18 cm here); ρ and η are the density and dynamic viscosity, respectively, of the liquid [ρ= 0.99336 g/ml (2) and η = 0.006915 poise (3) for water at 37°]; and $\bar{u}$ is the mean linear flow velocity of the liquid.

At the minimum solvent flow rate used—*viz.*, $\bar{u}$ = 0.79 cm/sec, $h_0 \approx$ 8.0 mm. At the maximum possible flow rate for streamline (laminar) flow (Re = 3000)—*viz.*, $\bar{u}$ = 6.7 cm/sec, $h_0 \approx$ 2.7 mm. The dimensions of dissolution chamber C were such that the surface and lateral edges of the potassium chloride disk were in the middle of the flow stream and 13 mm (1 disk diameter) from each wall of C. Now, 13 mm > h_0 throughout the range of streamline flow rates used or, in other words, the whole surface of the dissolving solid was outside the hydrodynamic boundary layer of the chamber wall and, therefore, at a position of uniform approach velocity. Clearly, the presence of any object in the dissolution chamber will modify these otherwise ideal flow conditions.

The dissolving solid, F, was held at the center of dissolution chamber C in such a manner as to minimize the disturbance of the uniform flow pattern (Fig. 2). Accordingly, mounting stub D was oriented downstream from F and below the level of the solid surface; F was surrounded by ring K to protect its edges and to enable it to be mounted within an IR absorption spectrophotometer for future work. The thickness, annular area, and composition of ring K and the circular shape of dissolving solid F enabled F to be formed under pressure (Fig. 1) without distortion of the ring or fracture of F. The edges of ring K were rounded to give the least interference with the flow pattern within the dissolution chamber. All these factors contributed to reproducibility (feature *g*).

The solvent flowed from elevated reservoirs at the constant predetermined rate through an on–off valve and a fine control valve to inlet tube A (Fig. 2). The solvent then flowed upward through the apparatus. The dissolution apparatus and the solvent reservoirs were surrounded by thermostatically controlled water baths at 37.0 ± 0.1°. The water bath containing the dissolution apparatus had a glass front to permit observation of the disk.

Each dissolution run was begun with the solvent level just below the potassium chloride disk. The liquid from C passed through a cone of decreasing diameter to the narrow outlet tube, G. Samples were collected from G at 10-sec intervals in weighed flasks until part of the disk had been eroded (after 2–4 min). The flasks were reweighed and, from the mass of solution collected in each time interval, the mean volume flow rate, dV/dt, was calculated assuming that the density, ρ, of the solution, which was very dilute, was equal to that of pure water, *i.e.*, 0.99336 g/ml at 37° (2). The effluent solution was analyzed for dissolved potassium chloride. Samples taken from different regions of each effluent solution contained the same concentration of potassium chloride. This finding shows that mixing, which took place between C and G, was adequate (feature *b*).

Analysis—The concentration of potassium chloride dissolved in the effluent solution was determined as potassium ions by means of a flame photometer[3].

Calculation of Dissolution Rate—At a given instant in time t, let the volume of solution within the dissolution chamber be V, let this solution contain a mass, m, of solute dissolved from the solid disk, and let the mean concentration of solute within the dissolu-

[3] Evans Electroselenium Ltd., St. Andrews Works, Halstead, Essex, England.

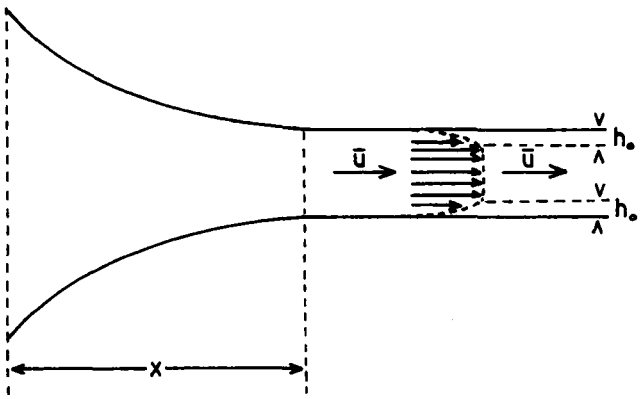

Figure 3—*Velocity distribution across a pipe (shown by horizontal arrows) when flow through the pipe is preceded by an exponentially shaped horn of length* x. *The mean linear velocity through the pipe is* ū, *and the thickness of the hydrodynamic boundary layer is* h_0.

tion chamber be c. In an infinitesimal interval of time, the solution in the chamber gains mass dm of solute from the dissolving solid and, in volume dV of effluent, it loses mass $c(dV)$ of solute.

In the present continuous-flow dissolution apparatus, there is no accumulation of solute within the dissolution chamber. Consequently, the gain in solute mass dm is exactly balanced by the loss in solute mass $c(dV)$, so that:

$$dm = c(dV) \qquad \text{(Eq. 2)}$$

and the concentration of solute in any sample of the effluent after thorough mixing gives a direct measure of c. If dt represents the infinitesimal time interval referred to:

$$\frac{dm}{dt} = c\frac{dV}{dt} \qquad \text{(Eq. 3)}$$

where dm/dt is the overall dissolution rate of the solid disk, and dV/dt is the overall solvent flow rate (*i.e.*, the rate of increase in effluent volume).

The intrinsic dissolution rate is defined as the dissolution rate per unit area. The dissolution rate may exhibit different values for each small element of surface of the dissolving solid. For practical purposes, the overall intrinsic dissolution rate, G, of the dissolving solid is taken to be:

$$G = \left(\frac{dm}{dt}\right)\left(\frac{1}{A}\right) \qquad \text{(Eq. 4)}$$

where dm/dt is the overall dissolution rate, and A is the total area of the dissolving solid exposed to the solvent (A = 1.3272 cm^2). Combining Eqs. 3 and 4 gives:

$$G = \left(\frac{c}{A}\right)\left(\frac{dV}{dt}\right) \qquad \text{(Eq. 5)}$$

from which G was calculated.

Calculation of Reynolds Number for Solvent Flow—The parameter used to represent solvent flow was the dimensionless grouping, Reynolds number, Re, which is given by:

$$Re = \frac{\rho\, du}{\eta} \qquad \text{(Eq. 6)}$$

where ρ is the density, and η is the dynamic viscosity of the solution. Since the solution was dilute, these values were taken to be the same as those for pure water, *i.e.*, ρ = 0.99336 g/ml (2) and η = 0.006915 poise (3) at 37°. The mean hydraulic diameter, d, of the rectangular chamber was given by four times the cross-sectional area divided by the wetted perimeter: $d = 4 \times 10.14$ cm^2/13 cm = 3.12 cm.

The linear flow rate, u, was given by dV/dt divided by the cross-sectional area of the dissolution chamber, 10.14 cm^2. Thus:

$$Re = 44.20\ (\text{sec/cm}^3) \times \frac{dV}{dt}\ (\text{in cm}^3/\text{sec}) \qquad \text{(Eq. 7)}$$

from which Re was calculated for each flow rate (feature *a*).

Visualization of Solvent Flow—Two methods of flow visualization were used. One was to pass aqueous 2 M $AgNO_3$ solution over a potassium chloride disk and to examine the resulting white colloidal solution of silver chloride. The other method was to incorporate 1 mg of gentian violet into a potassium chloride disk and to study the color pattern as the disk dissolved. The latter method was less satisfactory because initially very small particles of gentian violet tended to fall a few millimeters downward before being swept forward by the solvent.

RESULTS

Visualization of Solvent Flow—The white colloid silver chloride formed in the first method left the disk at right angles to the surface and changed direction a few millimeters from it. At Re < 360, the silver chloride flowed downward against the stream of flowing solvent, showing that back-convection was taking place. At Re > 360, the silver chloride flowed upward with the solvent stream. At Re < 3000, flow of silver chloride appeared laminar (or streamline). The second method of flow visualization using gentian violet gave similar results.

Effect of Reynolds Number for Water Flow on Intrinsic Dissolution Rate of Potassium Chloride—The concentration, c, of potassium chloride in the effluent (*e.g.*, in Fig. 4) was practically constant as long as the area, A, of the disk appeared constant (feature *d*). The coefficient of variation of the steady-state concentration during a run was about 6%. Initially, c was lower than the mean value, presumably because the steady state had not been attained. After about 120 sec, c decreased, since the disk began to be eroded and its area decreased thereafter. No matter what the flow rate, erosion commenced at the downstream edge of the disk, revealing the underlying metal stub.

The mean steady-state value of c decreased with increasing Re but fluctuated for Re > 3000. The highest recorded value of c (at Re = 367) was 0.153 g of potassium chloride/liter; this concentration was less than c_s by a factor of about 2000, where c_s is the solubility of potassium chloride in water at 37° (334 g/liter) (4). Thus, $c \ll c_s$, *i.e.*, $(c_s - c) \approx c_s$, as required (feature *c*).

At Re < 360, the system gave inconsistent results due to back-convection of the denser, concentrated solution formed in the immediate vicinity of the disk. This finding was proved by analysis of the liquid remaining in the base of the apparatus (B in Fig. 1) after a disk dissolved completely. At Re > 360, no back-convection was observed.

Figure 5 shows the effect of Re on G. At Re < 3000, *i.e.*, for streamline flow and in the transition region, G was a linear function of Re; thus:

$$G(\text{in g/m}^2\,\text{sec}) = 8.805 + 0.001414\,Re \qquad \text{(Eq. 8)}$$
$$r = 0.993 \qquad s^2 = 0.0235$$

where r is the correlation coefficient, and s^2 is the residual variance of the G values. In the region of definite turbulent flow, *i.e.*, at Re > 3000, values of G fluctuated about the mean regression line. This scatter was induced by turbulence. The linear regression line, calculated by giving equal weight to each result in the streamline, transition, and turbulent regions, was:

$$G(\text{in g/m}^2\,\text{sec}) = 8.820 + 0.001383\,Re \qquad \text{(Eq. 9)}$$
$$r = 0.981 \qquad s^2 = 2.46$$

Comparison of Eqs. 8 and 9 shows that inclusion of results at Re >

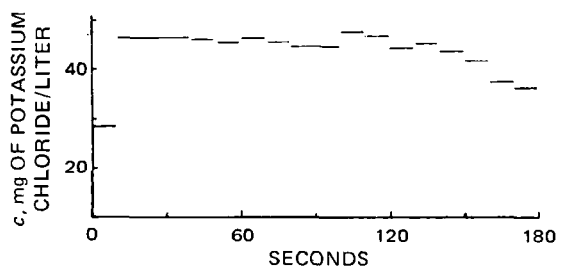

Figure 4—*Time dependence of the concentration of potassium chloride in the effluent of the dissolution apparatus from a disk of potassium chloride.*

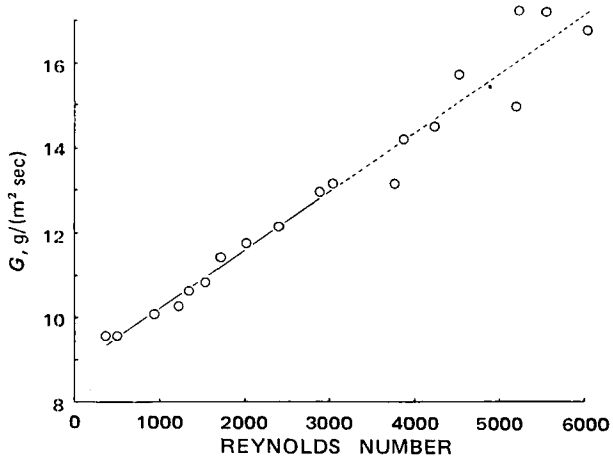

Figure 5—*Effect of Reynolds number for solvent flow on the intrinsic dissolution rate, G, of compressed disks of potassium chloride.*

3000 has little effect on the constants in the relationship between G and Re, but the greater fluctuation of points in the turbulent region is reflected in a much greater residual variance and in a slightly lower correlation coefficient.

When different potassium chloride disks were prepared and dissolved by the same or a different operator using the procedure described at Re = 1335, values of the mean steady-state concentration and G did not differ from disk to disk or from operator to operator by more than 2%. This finding indicates the high degree of reliability and reproducibility of the technique (feature *e*).

DISCUSSION

Dissolution Apparatus—The features required of the dissolution apparatus were achieved. The only limitation was back-convection of solute at $Re < 360$. The solvent flow rate under these conditions was insufficient to sweep forward all of the concentrated solution formed at the disk surface. In other respects, the apparatus and technique were satisfactory.

Disk Erosion—The upper (or downstream) segment of the disk was eroded preferentially. According to the theory of Levich (5) for a plate in a parallel stream of reactive liquid, the diffusional flux (*i.e.*, the intrinsic dissolution rate) at the upstream edge of the plate is greater than at the downstream edge. Thus, the asymmetric pattern of erosion of the solid in the present system differs from the theory. A possible reason for this difference may be that the metal ring surrounding the disk, although rounded, slightly disturbs the flow profile around the dissolving solid.

Reaction-Controlled Dissolution Models—These models are exemplified by the interfacial barrier model of Higuchi (6) and the theory of Szinai and Hunt (7). According to the former model:

$$G = k_i(c_s - c) \qquad \text{(Eq. 10)}$$

where k_i is known as the "effective interfacial transport rate constant." By introducing $(c_s - c) \approx c_s$ = 0.33414 g/ml (4) and expressing G in terms of Re (Eq. 9), k_i is found to be the following function of Re:

$$k_i(\text{in cm/sec}) = 0.00264 + (4.14 \times 10^{-7}\, Re) \qquad \text{(Eq. 11)}$$

Diffusion-Controlled Dissolution Models—According to the model of Danckwerts (8), which was originally developed for the dissolution of gases and has since been applied to the dissolution of solids (6), G is given by:

$$G = \sqrt{DS}\,(c_s - c) \qquad \text{(Eq. 12)}$$

where D is the integral diffusion coefficient of the solute from its saturated solution to pure water, and S is a constant known as the "mean rate of production of fresh surface." The term D was evaluated by extrapolating the integral diffusion coefficient of potassium chloride in water (9, 10) to c_s = 334.14 g/liter (4) at 37°. By introducing $D = 3.22 \times 10^{-5}$ cm²/sec so obtained and the value of c_s, assuming sink conditions, and expressing G in terms of Re (Eq. 9),

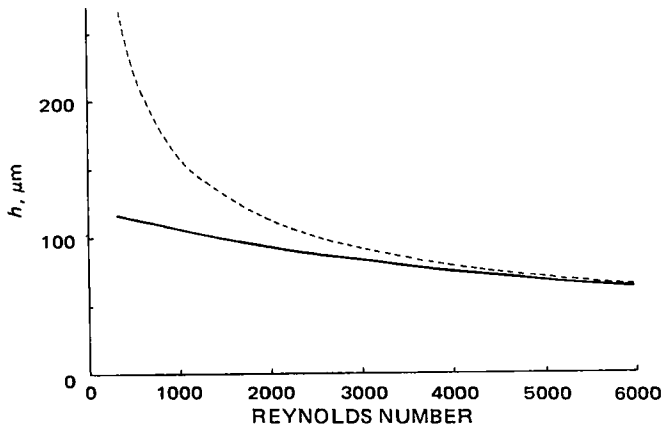

Figure 6—*Effect of Reynolds number for solvent flow on the thickness, h, of the diffusion layer for the dissolution of potassium chloride in water. Key: —, calculated from the experimental values of G by means of Eq. 14; and - - -, calculated from the physical constants of the system using Eq. 16.*

S is given as the following function of Re:

$$S(\text{in 1/sec}) = [0.465 + (7.30 \times 10^{-5}\, Re)]^2 \qquad \text{(Eq. 13)}$$

According to the diffusion layer model (11, 12):

$$G = \frac{D}{h}(c_s - c) \qquad \text{(Eq. 14)}$$

where h is the thickness of the diffusion layer. Introducing these values of D and c_s, assuming sink conditions, and expressing G in terms of Re (Eq. 9) give:

$$h = \frac{122.0\ \mu\text{m}}{1 + (1.568 \times 10^{-4}\, Re)} \qquad \text{(Eq. 15)}$$

This relationship between h and Re is expressed graphically as the lower curve in Fig. 6. Over the range of Reynolds numbers investigated, the thickness, h, of the diffusion layer was 60–110 μm, two to three times that found for other solid–liquid dissolution systems (12–14). The exceptionally high value of h may arise from the high solubility of potassium chloride, which would otherwise lead to very high concentration gradients near the solid surface.

Levich (5) derived the following equation for h in terms of fundamental physical quantities for nonturbulent (or laminar) flow along a flat disk, provided that the dimensions of the system are such that other wall and edge effects are negligible:

$$h = 3x^{1/2}D^{1/3}\nu^{1/6}u^{-1/2} \qquad \text{(Eq. 16)}$$

where D is the diffusion coefficient of the solute (3.22×10^{-5} cm²/sec, as before), ν is the kinematic viscosity of the solvent ($\eta/\rho = 6.961 \times 10^{-3}$ cm²/sec or stokes), x is the distance from the up-

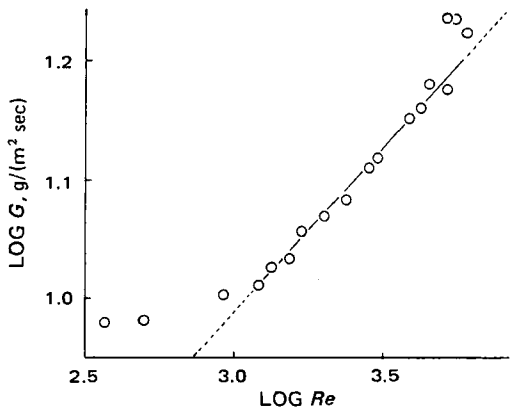

Figure 7—*Relationship between the logarithm of the intrinsic dissolution rate, G, of potassium chloride in water and the logarithm of the Reynolds number, Re, for solvent flow. This figure is a log–log plot of the data in Fig. 5.*

stream edge of the disk measured along an axis parallel to the direction of flow, and u is the characteristic linear flow velocity of the system (taken as the mean value), which is given by Eq. 6. By substituting the numerical values of η, ρ, and d previously quoted, the following expression for u is obtained:

$$u(\text{in cm/sec}) = 0.002231\,Re \qquad \text{(Eq. 17)}$$

The mean value of x along a line passing through the center is taken to be equal to the radius of the disk (0.650 cm), whereas it is zero at the extreme left-hand and right-hand sides of the disk. The mean value of x over the whole disk is probably close to the mean of these values, 0.325 cm. By substituting into Eq. 16 the numerical values previously quoted and the expression for u in terms of Re, the following expression for h in terms of Re is obtained:

$$h(\text{in } \mu\text{m}) = 5033\,Re^{-1/2} \qquad \text{(Eq. 18)}$$

The Levich equation (Eq. 16) was derived for a uniform plate that reacts with the solvent over its entire area, so that at its leading (or upstream) edge the thickness of the hydrodynamic boundary layer, h_0, and that of the diffusion boundary layer, h, are both zero. In the present work, the dissolving disk (F in Fig. 2) is surrounded by a chemically inert annular ring, K, such that the leading edge of the dissolving disk is 4 mm downstream from the hydrodynamic edge.

However, Eq. 16 is derived by considering the momentum balance on a control volume of fluid and assumes that the change of momentum within a given layer equals the retarding force due to the wall shear stress. This assumption is still valid for the present system in which the diffusion boundary layer, h, begins at a different point from the hydrodynamic boundary layer, h_0. Thus, Eq. 16 is not itself modified by the thickness of the ring.

The asymmetric pattern of erosion of the disk, previously discussed, suggests that the annular ring (K in Fig. 2) modifies the flow profile over the surface of disk F, even though the flow visualization experiments indicate that this disturbance is insufficient to create turbulence at $Re < 2000$. Therefore, the present system deviates markedly from the Levich theory as a result of the influence of the solid disk and its holder.

The fact that Eq. 16 and, by implication, Eq. 18 are not strictly valid for turbulent flow may not itself cause significant deviations from the Levich theory, because flow near the surface of a solid tends to be laminar even though the bulk of the liquid may be turbulent (15).

The theoretical relationship between h and Re (Eq. 18), involving only the physical constants of the system, is expressed graphically in Fig. 6 and compared with Eq. 15 derived from the experimental relationship between G and Re (Eq. 9). If the approximations made in deriving Eq. 16 are considered, there is good agreement between the theoretical and experimental h values at high Re. This finding strongly suggests that the diffusion layer model operates at the higher flow rates, where forced convection predominates over natural convection. That the experimental values of h become progressively smaller than the theoretical value as Re is reduced suggests that natural convection becomes increasingly important the lower the flow rate and reflects deviations from the Levich theory.

According to Nernst (11), an increase in the rate of agitation of the dissolution medium should reduce h and increase the dissolution rate. This effect has been amply confirmed by experiment (12, 16–18) and is usually expressed as a power law:

$$\frac{dm}{dt} = aR^b \qquad \text{(Eq. 19)}$$

where R is the rate of agitation or stirring, and a and b are constants such that $b \leq 1$. For the present continuous-flow apparatus, $G \propto dm/dt$ and $R \propto Re$, so the power law may be written:

$$G = a(Re)^b \qquad \text{(Eq. 20)}$$

or:

$$\log G = \log a + b \log Re \qquad \text{(Eq. 21)}$$

where a is a new constant.

If dissolution is reaction controlled, R or Re should exert little or no influence on the dissolution rate and b should be close to zero. If dissolution is diffusion controlled, b should be significant. Levich (5) calculated that b should be close to 0.5 when flow is laminar ($Re < 2000$) and close to 1.0 for turbulent flow ($Re > 3000$). These calculations were confirmed experimentally for the dissolution of benzoic acid and iodine in water (17).

Figure 7 shows a log–log plot of the data in Fig. 5 and is approximately linear, indicating that Eqs. 20 and 21 are obeyed except at $Re < 1000$. Linear regression analysis of the data, omitting the three deviant points for $Re < 1000$ and all those for definite turbulent flow ($Re > 3000$), gives $a = 1.546$ g/m^2 sec and $b = 0.2667$ as best fitting Eq. 21, with the correlation coefficient being 0.995 and the residual variance of log G being 0.000017. If only the three deviant points at $Re < 1000$ are omitted, the constants that best fit Eq. 21 are $a = 1.117$ g/m^2 sec and $b = 0.3096$, with the correlation coefficient being 0.972 and the residual variance of log G being 0.000328.

The increase in gradient, b, brought about by turbulence accords with Levich's (5) predictions for the diffusion layer theory, but the actual values (~0.3) are lower than those (0.4–1.0) found by other workers (13, 16–18) for the dissolution of solids and other diffusion-controlled chemical processes. Thus, the present dissolution system is less sensitive to solvent flow than other examples.

The form of the log G–log Re plot in Fig. 7 is similar to that for the dissolution of salicylic acid in water studied by Travers and Powdrill (19), who deduced that natural convection was an important feature in their experiments. The predominance of natural convection over forced convection at low solvent flow rates explains the constancy of log G at the lowest log Re values (Fig. 7) as well as the fact that the experimental values of h were less than those calculated theoretically for forced convection (Fig. 6).

Natural convection is unlikely to be caused by temperature gradients, since the system is thermostatically controlled to ±0.1°, but it could well arise from variations in density due to concentration changes within the liquid phase. The importance of the latter effect was shown by the convection of the dense solution formed on dissolution at $Re < 360$ in a downward direction against the rising solvent stream.

CONCLUSIONS

The present apparatus achieved our objectives. By enabling the intrinsic dissolution rate to be determined at various Reynolds numbers, the method enables the unknown constant in any dissolution model with only one such constant to be expressed in terms of Re. Comparison of the thickness of the diffusion layer so determined with that calculated from the physical constants of the system, using Eq. 16 (5), provides a simple means of testing the applicability of the diffusion layer model.

Indeed, the present work indicates that the dissolution of potassium chloride in water agrees with the diffusion layer model when forced convection predominates over natural convection. The effect of viscosity of the medium on the dissolution rate (20) supports this model. In the present system, natural convection becomes increasingly important as the solvent flow rate is reduced.

REFERENCES

(1) V. L. Streeter, "Fluid Mechanics," McGraw-Hill, New York, N.Y., 1966.

(2) "Handbook of Chemistry and Physics," 53rd ed., Chemical Rubber Co., Cleveland, Ohio, 1972.

(3) G. W. C. Kaye and T. H. Laby, "Tables of Physical Constants," 13th ed., Longmans, London, England, 1966.

(4) W. F. Linke, "Solubilities: Inorganic and Metal Organic Compounds," 4th ed., vol. II, American Chemical Society, Washington, D.C., 1965.

(5) V. G. Levich, "Physicochemical Hydrodynamics," Prentice-Hall, Englewood Cliffs, N.J., 1962.

(6) W. I. Higuchi, *J. Pharm. Sci.*, **56**, 315(1967).

(7) S. S. Szinai and A. C. Hunt, *Can. J. Pharm. Sci.*, **7**, 78(1972).

(8) P. V. Danckwerts, *Ind. Eng. Chem.*, **43**, 1460(1951).

(9) R. H. Stokes, *J. Amer. Chem. Soc.*, **72**, 2243(1950).

(10) H. S. Harned and R. L. Nuttall, *ibid.*, **71**, 1460(1949).

(11) W. Nernst, *Z. Phys. Chem.*, **47**, 52(1904).

(12) E. Brunner, *ibid.*, **47**, 56(1904).

(13) L. L. Bircumshaw and A. C. Riddiford, *Quart. Rev. Chem.*

Soc., 6, 157(1952).
(14) A. Hussain, *J. Pharm. Sci.*, 61, 811(1972).
(15) A. Fage and H. C. H. Townend, *Proc. Roy. Soc. A*, 135, 656(1932).
(16) W. Nernst and E. S. Merriam, *Z. Phys. Chem.*, 53, 235(1905).
(17) S. Bisaillon and R. Tawashi, *J. Pharm. Sci.*, 60, 1874(1971).
(18) J. H. Collett, J. A. Rees, and N. A. Dickinson, *J. Pharm. Pharmacol.*, 24, 724(1972).
(19) D. N. Travers and A. Powdrill, *J. Pharm. Pharmacol., Suppl.*, 24, 153P(1972).
(20) A. B. Zdanovskii, *Zh. Fiz. Khim.*, 25, 170(1951); through *Chem. Abstr.*, 48, 4291c(1954).

ACKNOWLEDGMENTS AND ADDRESSES

Received September 30, 1974, from the *Department of Pharmacy, University of Nottingham, University Park, Nottingham, NG7 2RD, England.*

Accepted for publication April 7, 1975.

The authors are grateful to Mr. John Trigg and Dr. R. K. Duggins for valuable discussions concerning the design of the apparatus and to the Sheffield Regional Hospital Board for financial support for Miss J. Valerie Fee.

* Present address: Royal Infirmary of Edinburgh, Lauriston Place, Edinburgh, EH3 9YW, Scotland.

ˣ To whom inquiries should be directed.

Fluorocarbon Aerosol Propellants VIII: Solubility of Trichloromonofluoromethane in Dog Blood and Tissue Homogenates

KUN CHANG and WIN L. CHIOU ˣ

Abstract □ The solubility of trichloromonofluoromethane in dog blood and tissue homogenates was measured indirectly using the head-space method at 37°. These values, except that in dog blood, were used to estimate the solubility in the whole tissues or organs. In most cases, the solubility so obtained was independent of equilibrium concentration. However, a considerable concentration dependence for the solubility was observed in dog heart and kidney. The highest solubility found was in dog fat *versus* air, *i.e.*, 45.6, which is almost 220 times higher than the solubility in water or normal saline. Fat solubilization and specific binding interactions appeared to be the two major factors in determining the solubility. The pharmacokinetic implications of such findings are discussed.

Keyphrases □ Fluorocarbon aerosol propellants—solubility of trichloromonofluoromethane in dog blood and tissue homogenates □ Aerosol propellants—solubility of trichloromonofluoromethane in dog blood and tissue homogenates □ Propellants—solubility of trichloromonofluoromethane in dog blood and tissue homogenates □ Trichloromonofluoromethane—solubility in dog blood and tissue homogenates

The wide use of fluorocarbon aerosol propellants in various household, cosmetic, and medicinal pressurized packages recently prompted extensive studies on their possible adverse effects on the cardiovascular system (1–10), enzyme activities (7, 11–13), mutation (14), and ozone concentrations in the stratosphere (15, 16). The high apparent volume of distribution in dogs (17–19) and the moderate to extensive binding with both bovine and human albumins (20–23) of the three most commonly used fluorocarbon propellants prompted the investigation of their solubilities in various tissues and organs. The information obtained from such an investigation is essential to the construction of a physiologically based pharmacokinetic model as reported for barbiturates (24) and methotrexate (25). The results of the solubility study of trichloromonofluoromethane in blood and tissue homogenates of dogs are reported in this article.

For a gaseous or volatile compound, the solubility is commonly defined as the ratio of its concentration in the liquid phase to its concentration in the gaseous phase at the equilibrium state (19, 26, 27). Such a definition is analogous to that of the partition coefficient, P, which has been conventionally used to describe the distribution of a nonvolatile compound between two immiscible liquid phases. These two terms are used interchangeably in this article.

EXPERIMENTAL

Preparation of Samples—Three male mongrel dogs, 17–20 kg, were sacrificed and their tissues were separated, individually wrapped, and kept in a freezer. Prior to the homogenization of the lean tissue, all conspicuous attached fatty tissues were removed and the "clean" tissue was weighed and chopped. Then for each gram of the prepared tissue, 4 ml of chilled sodium chloride injection USP[1] was added and the mixture was homogenized in a blender[2].

The stock bottle[3] of trichloromonofluoromethane[4] (bp 23.82°) was prepared within a month of the experiment to minimize the rate of loss due to storage (28). The bottle had a nominal volume of 500 ml and a fluorocarbon concentration in the 0.64–0.96-mg/ml range.

Procedure—For the study of the partition coefficient of the propellant in each tissue, four pairs of 60-ml serum bottles were prepared. Each pair consisted of an empty control and a sample bottle into which 40 ml of the tissue homogenate was introduced with a 50-ml glass syringe. All bottles were sealed with lacquer-coated stoppers[5] and aluminum caps. They were then immersed in a water bath preset at 37° and shaken mechanically for 15 min.

This step was followed immediately by releasing the extra pressure developed in the bottles by inserting a syringe needle for a moment. Then a calculated amount of air was withdrawn from these bottles, which were expected to show significant pressure

[1] Sodium chloride injection USP, McGaw Laboratories, Division of American Hospital Supply Corp., Glendale, CA 91201
[2] Waring blender, Scientific Products, McGaw Park, IL 60085
[3] Wheaton serum bottle, Wheaton Scientific, Division of Wheaton Industries, Millville, NJ 08332
[4] Freon 11, E. I. du Pont de Nemours and Co., Wilmington, Del.
[5] Lacquer-coated rubber stopper, West Co., Phoenixville, Pa.